Journal of Hazardous Materials 219–220 (2012) 231–239

Contents lists available at SciVerse ScienceDirect

Journal of Hazardous Materials

journal homepage: www.elsevier.com/locate/jhazmat

# Modeling volatilization of residual VOCs in unsaturated zones: A moving boundary problem

Talib R. Abbas[a], Jung-Hau Yu[b], Chiu-Shia Fen[c], Hund-Der Yeh[b,*], Li-Ming Yeh[d]

[a] Water Treatment Technology Directorate, Ministry of Science and Technology, Baghdad, Iraq
[b] Institute of Environmental Engineering, National Chiao Tung University, Hsinchu, Taiwan
[c] Department of Environmental Engineering and Science, Feng Chia University, Taichung, Taiwan
[d] Department of Applied Mathematics, National Chiao Tung University, Hsinchu, Taiwan

ARTICLE INFO

*Article history:*
Received 18 October 2011
Received in revised form 24 March 2012
Accepted 31 March 2012
Available online 7 April 2012

*Keywords:*
Analytical solution
Finite difference model
NAPL
Vadose zone
VOC

ABSTRACT

It is of practical interest to investigate the natural evaporation of volatile organic compounds (VOCs) after the removal of a leaking tank situated on the top of the soil. This study aims to develop a mathematical model to predict mole fraction distributions and migration of evaporation front for two VOCs emanating from residual non-aqueous phase liquid (NAPL) due to the leak from the tank in a homogeneous soil. Considering the location of the front and the regions above and below the front, a numerical model for the diffusive transport of VOCs in unsaturated soils was developed using the finite difference method with a moving grid approach. The model was further simplified to the case of single VOC and solved analytically by Boltzmann's transformation with a moving boundary. Analytical expressions for the depth and moving speed of the front for a single VOC were then obtained for practical use. Finally, the developed model was used to predict the concentration distributions of VOCs below the land surface and examine the factors affecting the location and moving speed of the evaporation front.



## 1. Introduction

Subsurface contamination by volatile organic compounds (VOCs) has been one of important issues to environmental problems. Especially, the leak from an underground storage tank is an important source for the spill of VOCs in unsaturated soils. Once leak occurs, some VOCs may reside in soils as residual non-aqueous phase liquid (NAPL) [1,2]. Moreover, the VOCs may distribute among gas, liquid, and adsorbed phases in soils [3]. The transport mechanisms and fates of VOCs in unsaturated soils include advection, diffusion, dispersion, sorption, volatilization, interphase mass transfer, and chemical and biological reactions. Diffusion is generally the key mechanism under natural condition, especially, for gas transport in low-permeability soils. Most of the studies neglected advection for migration of organic vapors and gases in unsaturated soils [4–7]. Falta et al. [8] indicated that density driven advection is insignificant if the magnitude of soil permeability is less than $1 \times 10^{-11}$ m$^2$. Massmann and Farrier [9] mentioned that advection induced by atmospheric pressure fluctuation is not substantial for gas transport in unsaturated soil with permeabilities less than $1 \times 10^{-14}$ m$^2$ under normal weather conditions.

In the past, several mathematical models were developed to assess the fate and transport of VOCs in unsaturated soils [1,9–13] or in biological reactors [14]. Rivett et al. [15] presented a review of unsaturated zone transport and attenuation of plumes leached from shallow VOC source zones. Jury et al. [16] developed an analytical solution for a single pesticide species partitioning to gas, water and adsorbed phases undergoing first-order decay in an unsaturated soil. Later, Jury et al. [17] introduced an analytical model to evaluate the relative volatilization losses of some organic compounds under standard soil conditions. Lin and Hildemann [18] developed an analytical model including the mechanisms such as leachate flow, diffusion, adsorption, degradation, and volatilization to predict emissions of volatile organic compounds from hazardous or sanitary landfills. Shoemaker et al. [19] used the solution developed by Jury et al. [16] to study the effect of vapor phase sorption on the transport of organic compounds. Yates et al. [20] presented an analytical model to study the diffusion of organic vapors and other gases in layered soil systems. However, these models did not consider the existence of residual NAPL in soils and could underestimate the amounts of mass of VOCs residing in soil and migrating to the atmosphere. Sun et al. [21] developed an analytical solution for reactive transport of multiple volatile contaminants with assuming linear reaction kinetics and linear equilibrium partitioning between vapor, liquid, and solid phases in the unsaturated soil.

In unsaturated soils, the upper boundary of VOCs in NAPL while moving downward with time can be considered as an evaporation

* Corresponding author. Tel.: +886 3 5731910; fax: +886 3 5725958.
*E-mail address:* hdyeh@mail.nctu.edu.tw (H.-D. Yeh).

0304-3894/$ – see front matter © 2012 Elsevier B.V. All rights reserved.
http://dx.doi.org/10.1016/j.jhazmat.2012.03.082

**Nomenclature**

| | |
|---|---|
| $C$ | a constant parameter |
| $C_G$ | gas-phase concentration (kg/m$^3$) |
| $C_G^0$ | saturated gas concentration (kg/m$^3$) |
| $C_G^P$ | equilibrium gas concentrations of pure component (kg/m$^3$) |
| $C_L$ | liquid-phase concentration (kg/m$^3$) |
| $C_L^0$ | saturated liquid concentration (kg/m$^3$) |
| $C_L^P$ | equilibrium liquid concentrations of pure component (kg/m$^3$) |
| $C_S$ | adsorbed-phase concentration (dimensionless, kg/kg) |
| $C_S^0$ | saturated adsorbed concentration (dimensionless, kg/kg) |
| $C_T$ | total concentration (kg/m$^3$) |
| $C_T^0$ | saturated total concentration (kg/m$^3$) |
| $d$ | stagnant air boundary layer with thickness (m) |
| $D_E$ | effective diffusion coefficient (m$^2$/s) |
| $D_G$ | diffusion coefficient in gas phase in soil (m$^2$/s) |
| $D_G^{air}$ | diffusion coefficient in air (m$^2$/s) |
| $dt$ | time interval (day) |
| $dz$ | initial grid size (m) |
| $dz_{N-r}$ | grid size below the front (m) |
| $dz_r$ | grid size above the front (m) |
| $f$ | mass fraction of organic compound in NAPL |
| $f_{oc}$ | soil organic carbon fraction |
| $h$ | $D_G^{air}/d$ (m/s) |
| $i$ | number of component |
| $K_D$ | distribution coefficient (m$^3$/kg) |
| $K_H$ | Henry's law constant |
| $K_{oc}$ | organic carbon partition coefficient (m$^3$/kg) |
| $L$ | depth of lower boundary (m) |
| $M$ | molecular mass of the VOC (kg/mole) |
| $n$ | soil porosity |
| $P^0$ | saturated vapor pressure of the VOC (kPa) |
| $\Re$ | ideal gas constant (J/mole K) |
| $s$ | evaporation front (m) |
| $S_0$ | initial NAPL saturation |
| $S_G$ | saturation of gas-phase |
| $S_L$ | saturation of liquid-phase |
| $S_R$ | saturation of NAPL |
| $t$ | time (s) |
| $T$ | absolute temperature (K) |
| $u$ | mole fractions of organic compounds in the NAPL phase |
| $u_0$ | initial mole fraction |
| $U_f$ | moving speed of evaporation front (m/s) |
| $z$ | depth from surface (m) |
| $\delta_i$ | $\eta_i/D_G$ (s/m$^2$) |
| $\eta_i$ | $\phi S_G + (\phi S_W + \rho_b K_{Di})/K_H$ |
| $\theta_G$ | volumetric content of gas-phase |
| $\theta_G^0$ | initial volumetric content of gas-phase |
| $\theta_L$ | volumetric content of liquid-phase |
| $\theta_L^0$ | initial volumetric content of liquid-phase |
| $\theta_R$ | volumetric content of NAPL |
| $\theta_R^0$ | initial volumetric content of NAPL |
| $\mu_i$ | $\sigma_i M_i/D_G$ (kg s/mole m$^2$) |
| $\rho_b$ | soil bulk density (kg/m$^3$) |
| $\rho_R$ | density of NAPL (kg/m$^3$) |
| $\sigma_i$ | $\rho_R n/C_{Gi}^P$ |

front. The location of the front, considered as a moving boundary, changes with time [22]. Mostly, the phenomenon of moving boundary occurs in the problems of heat flow with phase changes and in some diffusion problems, e.g., [23–25].

The objective of this paper is to develop a model to predict the concentration distributions of VOCs as well as the migration of the evaporation front of NAPL with two VOCs after the removal of a leaking storage tank in a homogeneous unsaturated soil. To our knowledge, all the existing models for simulating the natural evaporation of NAPL VOCs in unsaturated soils employ specific boundary conditions at fixed boundaries in the problem domain. On the other hand, the present model considers the moving boundary in describing the downward movement of evaporation front of NAPL. The moving boundary divides the polluted area into two regions, i.e., the regions above and below the front. A numerical model is developed by the finite difference method with a moving grid approach for the location of the evaporation front and concentration distributions of two VOCs in these regions. The model is further simplified for a single VOC case and solved analytically using Boltzmann's transformation with a moving boundary. The prediction obtained from the analytical solution is then compared with those given by other analytical model and the developed numerical model for a single VOC case. In addition, analytical expressions developed from the analytical solution for the location and moving speed of the front are used to assess the time of vanish of NAPL at a specific location below the land surface.

## 2. Methods

### 2.1. Problem description

Fig. 1a shows a storage tank situated on the top of land surface and filled with VOCs. The VOCs, if leaking from the tank, exhibit four different phases (namely, gas, aqueous, adsorbed and residual NAPL phases) in the unsaturated soil. Assume that VOCs have equilibrium concentrations in these phases and the liquid phase is uniformly distributed in the soil with an initial NAPL saturation $S_0$. The saturation of each phase represents the volume percentage in the soil pore and the sum of saturation of each phase equals one. In addition, the evaporation front of the NAPL, denoted as $s(t)$, initially stays right at the land surface, i.e., $z = s(0) = 0$ where $z$ is the vertical axis and moves downward with time. Fig. 1b shows the scenario in which the gas phase VOCs begins to diffuse to atmosphere and the NAPL starts to vaporize to gas phase once the tank is removed. Assume that the NAPL evaporates fully above the front and the front migrates instantaneously when the evaporation occurs. Therefore, the NAPL saturation, $S_R$, equals zero between the land surface and the front and the residual NAPL still persists below the front.

### 2.2. Model formulation

Corapcioglu and Baehr [26] developed a mathematical model based on mass conservation for each VOC component in gas, water, adsorbed and NAPL phases in the unsaturated soil. Moreover, Baehr and Corapcioglu obtained a one-dimensional mass conservation equation [27, Eq. 1] for each VOC component based on following three assumptions: (1) both NAPL and air phases are immobile, (2) molecular diffusion of each VOC component within aqueous phase and NAPL is insignificant, and (3) abiotic transformation is negligible. By further neglecting biodegradation and gas phase advection and assuming that the water phase of VOC and NAPL are immobile, the equation of mass conservation for each VOC component in gas,

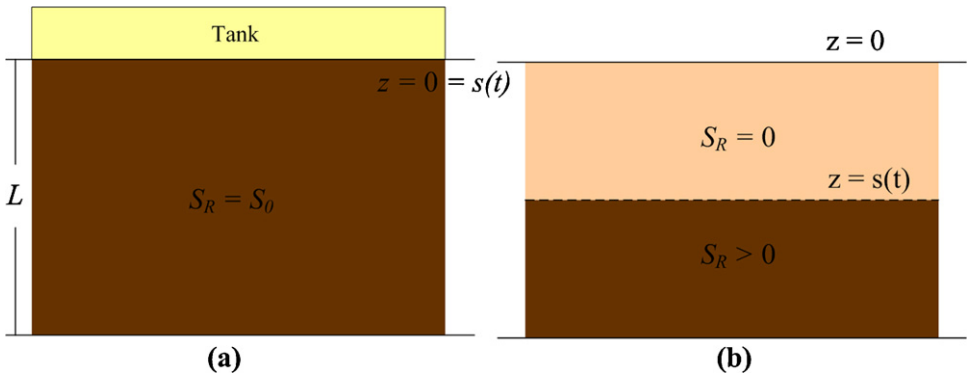


**Fig. 1.** Schematic diagram of VOC contamination problem where (a) VOCs reach equilibrium among each phase and (b) VOCs begin to evaporate after the tank is removed.

water, adsorbed and NAPL phases in the unsaturated soil with low permeability may be expressed as:

$$\frac{\partial C_{Ti}}{\partial t} - \frac{\partial}{\partial z}\left(\theta_G D_G \frac{\partial C_{Gi}}{\partial z}\right) = 0 \quad \text{for} \quad i = 1, \ldots, N_C \tag{1}$$

where $N_C$ is the total number of organic compounds; $C_{Ti}$, the total concentration of component $i$, is the sum of the concentration of each phase written as

$$C_{Ti} = C_{Gi}\theta_G + C_{Li}\theta_L + C_{Si}\rho_b + \rho_{Ri}\theta_R \tag{2}$$

where $C_{Gi}$, $C_{Li}$ and $C_{Si}$ represent the chemical concentrations in the gas, aqueous, and adsorbed phases of component $i$, respectively and $\rho_b$ and $\rho_{Ri}$ are the soil bulk density and liquid density of component $i$ in the NAPL, respectively. The symbols $\theta_G$, $\theta_L$ and $\theta_R$ are the volumetric contents of gas, aqueous and NAPL phases, respectively. They are denoted as

$$\theta_G = nS_G, \quad \theta_L = nS_L, \quad \text{and} \quad \theta_R = nS_R \tag{3}$$

where $n$ is the soil porosity and $S_G$, $S_L$ and $S_R$ are gas, water and organic liquid saturations, respectively.

The equilibrium relationships between the gas and aqueous phases as well as the aqueous and adsorbed phases may be expressed, respectively, as

$$C_{Gi} = K_{Hi}C_{Li} \quad \text{and} \quad C_{Si} = K_{Di}C_{Li} = K_{oci}f_{oc}C_{Li} \tag{4}$$

where $K_{Hi}$, $K_{Di}$ and $K_{oci}$ are Henry's Law constant, the distribution coefficient and the organic carbon partition coefficient, respectively, for component $i$ and $f_{oc}$ is the soil organic carbon fraction. The equilibrium relationships given in Eq. (4) are linear and reversible and their coefficients are dependent on chemical and soil properties.

$D_G$ in Eq. (1) is the soil-gas diffusion coefficient and usually assessed through the air-gas diffusion coefficient ($D_G^{air}$) multiplied by a tortuosity factor, which accounts for the reduced flow area and increased path length of diffusing molecules in the soil [28]. The relationship presented in Millongton and Quirk [29] is applied for the tortuosity factor [30]. Thus, $D_G$ is expressed as

$$D_G = D_G^{air}\left(\frac{\theta_G^{10/3}}{n^2}\right) \tag{5}$$

where the values of $D_G^{air}$ for different organic vapors are presumed the same in this study.

Substituting Eqs. (3) and (4) into Eq. (1), the mass-conservation equation of component $i$ for those four phases in the unsaturated soil becomes [31]

$$\eta_i \frac{\partial u_i}{\partial t} + \sigma_i \frac{\partial (S_R u_i M_i / \sum u_j M_j)}{\partial t} = D_G \frac{\partial^2 u_i}{\partial z^2} \quad i = 1, \ldots, N_C \tag{6}$$

where $\eta_i = nS_G + (nS_W + \rho_b K_{Di})/K_{Hi}$ and $\sigma_i = \rho_R n / C_{Gi}^p$ with $\rho_R$ being the total liquid density of the NAPL. In addition, $u_i$, the mole fraction of component $i$ in the NAPL, also represents the ratio of gas phase or water phase equilibrium concentrations of component $i$ for a NAPL mixture and a pure NAPL, i.e.,

$$C_{Gi} = u_i C_{Gi}^p \quad C_{Li} = u_i C_{Li}^p \tag{7}$$

$$\sum_{i=1}^{N_c} u_i = 1 \tag{8}$$

where $C_{Gi}^p$ and $C_{Li}^p$ are gas and water phase equilibrium concentrations of component $i$, respectively, for a pure NAPL. The saturated gas phase concentration for a pure NAPL can be estimated from the ideal gas law as

$$C_{Gi}^p = \frac{P_i^0 M_i}{\Re T} \tag{9}$$

where $P_i^0$ and $M_i$ are the saturated vapor pressure and the molecular mass of component $i$, respectively, $\Re$ is the ideal gas constant and $T$ is the absolute temperature.

### 2.3. Two-component model

The evaporation front, describing the upper boundary of the VOC evaporated from NAPL to gas phase, is naturally regarded as a moving boundary in the unsaturated soil. The problem domain for VOC transport with a moving boundary in the soil can therefore be divided into two regions: the one below the moving boundary and the other between the ground surface and the moving boundary. The transport equations for the mole fractions at the front and in those two regions in an unsaturated soil with two VOCs are discussed separately as follows:

#### 2.3.1. Below the evaporation front

In this region, NAPL phase persists and the saturation of NAPL is greater than zero, i.e., $S_R > 0$. Based on Eq. (6), the mass-conservation equation for two-component VOCs can be written as:

$$\eta_1 \frac{\partial u_1}{\partial t} + \sigma_1 \frac{\partial (S_R M_1 u_1 / (M_1 u_1 + M_2 u_2))}{\partial t} = D_G \frac{\partial^2 u_1}{\partial z^2} \tag{10}$$

$$\eta_2 \frac{\partial u_2}{\partial t} + \sigma_2 \frac{\partial (S_R M_2 u_2 / (M_1 u_1 + M_2 u_2))}{\partial t} = D_G \frac{\partial^2 u_2}{\partial z^2} \tag{11}$$

Eqs. (10) and (11) are constrained by Eq. (8); i.e., $u_1 + u_2 = 1$. If $u_1$ is selected as a primary variable, the saturation of NAPL can then be obtained from combining Eqs. (10) and (11) and making time integration as

$$S_R = \frac{[C - \delta_1 u_1 - \delta_2(1 - u_1)][M_1 u_1 + M_2(1 - u_1)]}{\mu_1 u_1 + \mu_2(1 - u_1)} \tag{12}$$

where $\delta_i = \eta_i/D_G$, $\mu_i = \sigma_i M_i/D_G$, and $C$ is a constant parameter which can be computed from the initial NAPL saturation, $S_0$, and the mole fraction of component 1, $u^0$, as:

$$C = \delta_1 u^0 + \delta_2(1-u^0) + S_0\frac{\mu_1 u^0 + \mu_2(1-u^0)}{M_1 u^0 + M_2(1-u^0)} \tag{13}$$

Substituting Eqs. (8) and (12) into Eq. (10) yields

$$\frac{\partial F(u_1)}{\partial t} = \frac{\partial^2 u_1}{\partial z^2} \tag{14}$$

where $F(u_1) = \delta_1 u_1 + \mu_1 u_1[C - \delta_1 u_1 - \delta_2(1-u_1)]/[\mu_1 u_1 + \mu_2(1-u_1)]$.

Eq. (14) has a lower boundary condition at depth $L$ expressed as

$$u_1(L,t) = u^o, \quad u_2(L,t) = 1 - u^o \tag{15}$$

where $L$ is the thickness of the contaminated soil zone.

*2.3.2. Above the evaporation front*

In this region the NAPL fully evaporates, i.e., $S_R = 0$. Eq. (6) can then be written for each component as:

$$\delta_1\frac{\partial u_1}{\partial t} = \frac{\partial^2 u_1}{\partial z^2} \tag{16}$$

$$\delta_2\frac{\partial u_2}{\partial t} = \frac{\partial^2 u_2}{\partial z^2} \tag{17}$$

where $u_1$ and $u_2$ are now the normalized concentration with respect to the vapor phase concentration for component 1 and 2, respectively, at the front.

The upper boundary condition specified at the ground surface can be simply expressed as

$$u_1(0,t) = u_2(0,t) = 0 \tag{18}$$

Eq. (18) presumes a condition that the VOC vapors migrating to ground surface immediately dilute with the atmosphere air.

*2.3.3. At the evaporation front*

Assume that the evaporation of the NAPL occurs instantaneously at the front and the mole fraction of each component is still governed by Eq. (8). Combining Eqs. (10) and (11), the equation for mass conservation at the front is obtained as

$$\frac{\partial S_R}{\partial t} = \left(\frac{D_G}{\sigma_1}\right)\frac{\partial^2 u_1}{\partial z^2} + \left(\frac{D_G}{\sigma_2}\right)\frac{\partial^2 u_2}{\partial z^2} - \left(\frac{\eta_1}{\sigma_1}\right)\frac{\partial u_1}{\partial t} - \left(\frac{\eta_2}{\sigma_2}\right)\frac{\partial u_2}{\partial t} \tag{19}$$

Using small time increment ($\Delta t$) and vertical grid size ($\Delta z$), Eq. (19) describing the front can then be written as

$$\lim_{\Delta t\to 0}\frac{0 - S_R^{t-} + (\eta_1/\sigma_1)(u_1^{t+} - u_1^{t-}) + (\eta_2/\sigma_2)(u_2^{t+} - u_2^{t-})}{\Delta t} = \lim_{\substack{\Delta s\to \frac{ds}{dt}\cdot\Delta t \\ \Delta t\to 0}}\frac{(D_G/\sigma_1)((\partial u_1^{z+}/\partial z) - (\partial u_1^{z-}/\partial z)) + (D_G/\sigma_2)((\partial u_2^{z+}/\partial z) - (\partial u_2^{z-}/\partial z))}{\Delta s} \tag{20}$$

where $s$ denotes the location of the moving front which changes with time, i.e., $s(t)$, as depicted in Fig. 1a; the superscripts $t+$ and $t-$ of the mole fraction denote the mole fractions at the time slightly after and before the vanish of NAPL, respectively, and $z+$ and $z-$ represent the mole fraction at the region slightly below and above the front, respectively. Eq. (20) can further be rearranged as

$$\frac{ds}{dt} = \frac{(D_G/\sigma_1)((\partial u_1^{z+}/\partial z) - (\partial u_1^{z-}/\partial z)) + (D_G/\sigma_2)((\partial u_2^{z+}/\partial z) - (\partial u_2^{z-}/\partial z))}{(\eta_1/\sigma_1)(u_1^{t+} - u_1^{t-}) + (\eta_2/\sigma_2)(u_2^{t+} - u_2^{t-}) - S_R^{t-}} \tag{21}$$

where $ds/dt$ represents the moving speed of the front.

As depicted in Fig. 1, the initial NAPL saturation is considered uniformly distributed in the soil and the mole fraction of each component is constant; they are

$$S_R(z,0) = S_0 \tag{22}$$

$$u_1(z,0) = u^o, \quad u_2(z,0) = 1 - u^o \tag{23}$$

In addition, the location of the evaporation front is initially located at the land surface and thus denoted as

$$s(0) = 0 \tag{24}$$

*2.4. Finite difference approximation*

The equations for describing the mass transport of VOCs at the front and in the regions below and above the front are solved separately by the finite difference method. An interpolative moving grid approach used by Javierre et al. [32] is adopted to handle this moving boundary problem. The total number of nodes within the problem domain is equal to $N$ and the nodal number assigned at the evaporation front starting from the land surface is designated as $r$. Accordingly, the number of grids from the land surface to the front is $r-1$, the number of grids below the front is $N-r$, and the initial grid size $dz$ is equal to $L/(N-1)$. The grid sizes above and below the front defined as $dz_r$ and $dz_{N-r}$, respectively, need to be re-adjusted after each move of the front. To avoid introducing large truncation error, the grid sizes $dz_r$ and $dz_{N-r}$ should be close to $dz$. If the front moves to a location between the nodal numbers initially assigned as $j$ and $j+1$, the new grid sizes of $dz_r$ and $dz_{N-r}$ are then calculated by $s/(r-1)$ and $(L-s)/(N-r)$, respectively, where $r = j+1$. The backward difference in time and central difference in space of finite difference formulas are used to discretize the governing equations of the proposed model. The difference equation of Eq. (14) for the mole fraction in the region below the front is therefore written as

$$\frac{F(u_{1j}^m) - F(u_{1j}^{m-1})}{dt} = \frac{u_{1(j+1)}^m - 2u_{1j}^m + u_{1(j-1)}^m}{(dz_{N-r})^2}, \quad s(t) < z \le L \tag{25}$$

where $m$ is the number of time step and $dt$ is the time interval. Once $u_1^m$ is solved, $u_2^m$ can be obtained from Eq. (8). The difference equations of Eqs. (16) and (17) for the mole fractions of the two components in the region above the front are, respectively,

$$\delta_1\frac{u_{1j}^m - u_{1j}^{m-1}}{dt} = \frac{u_{1(j+1)}^m - 2u_{1j}^m + u_{1(j-1)}^m}{(dz_r)^2}, \quad 0 \le z < s(t) \tag{26}$$

$$\delta_2\frac{u_{2j}^m - u_{2j}^{m-1}}{dt} = \frac{u_{2(j+1)}^m - 2u_{2j}^m + u_{2(j-1)}^m}{(dz_r)^2}, \quad 0 \le z < s(t) \tag{27}$$

Finally, the difference equations for the mole fractions of the two components at the front are also obtained from Eqs. (16) and (17) with different grid sizes above and below the front, respectively, and expressed as

$$\left(\frac{\delta_1}{2}\right)\frac{u_{1r}^m - u_{1r}^{m-1}}{dt} = \frac{dz_r u_{1(r+1)}^m + dz_{N-r}u_{1(r-1)}^m - (dz_r + dz_{N-r})u_{1r}^m}{(dz_r + dz_{N-r})dz_r dz_{N-r}}, \quad z = s(t) \tag{28}$$

$$\left(\frac{\delta_2}{2}\right)\frac{u_{2r}^m - u_{2r}^{m-1}}{dt} = \frac{dz_r u_{2(r+1)}^m + dz_{N-r} u_{2(r-1)}^m - (dz_r + dz_{N-r})u_{2r}^m}{(dz_r + dz_{N-r})dz_r dz_{N-r}}, \quad z = s(t) \tag{29}$$

Substituting Eq. (8) into Eq. (21), the difference equation for the change of front location can then be obtained as

$$\frac{s^m - s^{m-1}}{dt} = \frac{\frac{D_G}{\sigma_1}(((u_{1(r+1)}^m - u_{1r}^m)/dz_{N-r}) - ((u_{1r}^m - u_{1(r-1)}^m)/dz_r)) + (D_G/\sigma_2)(((u_{1r}^m - u_{1(r+1)}^m)/dz_{N-r}) - ((1 - u_{1r}^m - u_{2(r-1)}^m)/dz_r))}{(\eta_1/\sigma_1)(u_{1r}^m - u_{1r}^{m-1}) + (\eta_2/\sigma_2)(u_{1r}^{m-1} - u_{1r}^m) - S_R^{m-1}} \tag{30}$$

Procedure for determining the change of front location and the mole fraction of each component in regions above and below the front is described below:

1. Give the initial location of the front (Eq. (24)) and nodal values of mole fraction based on the initial conditions (Eqs. (22) and (23)) and boundary conditions (Eqs. (18) and (15)).
2. Guess a front location for a new time step after the start of evaporation.
3. Determine the nodal number for the front and the grid sizes based on the front location.
4. Solve the mole fraction of each component for the region below the front (Eq. (25)), for the region above the front (Eqs. (26) and (27)) and at the front (Eqs. (28) and (29)).
5. Compute the front location based on Eq. (30) with the mole fractions obtained in step 4.
6. Proceed to next time step if the difference between two succeeding guessed or computed locations of the front is less than a very small value, e.g., $10^{-10}$ m; otherwise, use the front location computed in step 5 to be the new guessed value and then go back to step 3.

### 2.5. Analytical solution for single VOC

The solution for single VOC can be developed analytically after simplifying the governing equations presented before. The problem domain is also divided into two regions based on the front location. In a homogeneous and unsaturated soil, the mass transport of a single VOC in a soil is described by Eq. (1) with *Nc* equal to one in which equilibrium relationship for mass distribution of the component among gas, water, NAPL and adsorbed phases is assumed, i.e., Eqs. (2), (4), (7) and (8).

In the region below the evaporation front, the NAPL has not been totally vaporized to gas phase yet. The VOC concentrations in gas and water phases are in saturation, i.e., $C_G^P$ and $C_L^P$, without having the subscript 1 for simplicity.

In the region above the evaporation front, the NAPL completely vaporizes to gas phase; therefore, the VOC is present only in gas, aqueous, and adsorbed phases. Eq. (1) without the subscript *i* can then be expressed as

$$\frac{\partial C_T}{\partial t} - D_E\frac{\partial^2 C_T}{\partial z^2} = 0 \tag{31}$$

where $C_T$ becomes the chemical concentration of a pure NAPL in the soil. $D_E = D_G/R_G$ denotes as effective diffusion coefficient and $R_G = \theta_G + \theta_L/K_H + \rho_b K_D/K_H$. Eq. (31) describes the vapor phase VOC transport between the land surface and the evaporation front. The boundary condition at the land surface is expressed as

$$C_T(0, t) = 0 \tag{32}$$

At the front, the volumetric content of water phase and the total soil porosity are assumed unchanged. In addition, the volumetric content of NAPL becomes the content of gas phase totally when the NAPL vaporizes to gas phase. By definition, $n = \theta_G + \theta_R + \theta_L$ in which $\theta_L$ is a constant; thus,

$$\frac{\partial \theta_G}{\partial t} = -\frac{\partial \theta_R}{\partial t} \tag{33}$$

It is common to assume that the bulk density $\rho_b$ does not change with time, i.e., $\partial\rho_b/\partial t = 0$. Therefore, taking the derivative of Eq. (2) with respect to time on both sides results in

$$\frac{\partial C_T}{\partial t} = (\rho_R - C_G^P)\frac{\partial \theta_R}{\partial t} \tag{34}$$

With Eq. (34) and after taking the limits of $\Delta t \to 0$ and $\Delta z \to 0$ for the differential terms in Eq. (1), the equation describing the VOC transport at the front becomes

$$\lim_{\Delta t\to 0}(\rho_R - C_G^P)\frac{\theta_R^{t+} - \theta_R^{t-}}{\Delta t} = \lim_{\Delta z\to 0}\frac{D_E((\partial C_T^{z+}/\partial z) - (\partial C_T^{z-}/\partial z))}{\Delta s} \tag{35}$$

If the volatilization occurs instantaneously, $\theta_R^{t+}$ equals the initial volumetric content of the NAPL ($\theta_R^0$) and $\theta_R^{t-}$ equals zero after evaporation. Below the front, the VOC concentration in each phase is the initial saturated concentrations; thus, the concentration gradient in gas phase below the front is naturally equal to zero, i.e., $\partial C_G^{z+}/\partial z = 0$. Since the liquid density of chemical is greater than the gas phase concentration about three orders ([9], Tables 1 and 4), the term related to $C_G^P$ on the left-hand side of Eq. (35) is thus negligible. Accordingly, the equation describing the location of the moving speed of the evaporation front $z = s(t)$ can be obtained from Eq. (35) as

$$\theta_R^0\rho_R\frac{ds}{dt} = D_E\frac{\partial C_T^-}{\partial z} \tag{36}$$

In summary, the mathematical model describing the vapor phase transport for a single VOC between the evaporation front and land surface consists of Eq. (31) as the governing equation and Eqs. (32) and (36) as the upper and lower boundary conditions, respectively.

Based on Boltzmann's transformation, a new variable is defined as $\xi = z/2\sqrt{D_E t}$. Eq. (31) can then be transformed to an ordinary differential equation as

$$\frac{d^2 C_T}{d\xi^2} + 2\xi\frac{dC_T}{d\xi} = 0 \tag{37}$$

The solution of Eq. (37) can be expressed as [33]

$$C_T(\xi) = A \cdot erf(\xi) + B \tag{38}$$

where $erf(\xi)$ is the error function and $A$ and $B$ are unknown coefficients. The variable $\xi = 0$ when $z = 0$. With the boundary condition of Eq. (32), Eq. (38) reduces to

$$C_T(z, t) = A \times erf\left(\frac{z}{2\sqrt{D_E t}}\right), \quad 0 < z < s(t) \tag{39}$$

The location of the front may be expressed as

$$s(t) = \alpha\sqrt{t} \tag{40}$$

where $\alpha$ is an unknown constant depending upon the characteristics of soil and the VOC. At the front, the total concentration is equal

**Table 1**
Soil properties used in the evaluation of model performance.

| Property | Symbol | Value |
|---|---|---|
| Soil porosity | $n$ | 0.4 |
| Initial NAPL saturation | $S_R^0$ | 0.01 |
| Initial water saturation | $S_I^0$ | 0.3 |
| Initial gas saturation | $S_G^0$ | 0.69 |
| Air diffusion coefficient ($m^2/s$)[a] | $D_G^{air}$ | $5 \times 10^{-6}$ |
| Temperature (°C) | $T$ | 20 |
| Soil organic carbon fraction | $f_{oc}$ | 0.0125 |
| Soil bulk density ($g/m^3$) [a] | $\rho_b$ | $1.59 \times 10^6$ |
| Depth of the lower boundary (m) | $L$ | 5 |

[a] Cited from [17].

to the initial total concentration, i.e., $C_T = C_T^0$. Thus, coefficient $A$ can be determined from Eqs. (39) and (40) as

$$A = \frac{C_T^0}{erf(\alpha/2\sqrt{D_E})} \tag{41}$$

Substituting Eqs. (39)–(41) into Eq. (36) yields

$$\frac{\theta_R^0 \rho_R \alpha}{2} = \frac{D_E C_T^0 \exp(-(\alpha^2/4D_E))}{\sqrt{\pi D_E} erf(\alpha/2\sqrt{D_E})} \tag{42}$$

The unknown constant $\alpha$ can then be easily determined from Eq. (42) by Newton's method [34]. In addition, the moving speed of the evaporation front ($U_f$) can also be obtained by taking the derivative of Eq. (40) with respect to time and the result is

$$U_f = \frac{\alpha}{2\sqrt{t}} \tag{43}$$

which may also represent the evaporation rate of a pure NAPL in soil.

### 2.6. Model performance

Leaks of petroleum fuels are often associated with aromatic hydrocarbons such as benzene, toluene, ethyl benzene, and various xylene isomers (BTEX). The benzene and toluene are chosen to simulate their transport in the unsaturated soil using the two-component model. In the past, carbon tetrachloride was commonly used as coolant in industry or produced as the fire extinguishers. This chemical is highly toxic and a small amount of it residing in soils may pose severe environmental problems. The carbon tetrachloride in the unsaturated soil is considered as in a pure state and analyzed using the analytical solution.

The performance of the present model is examined by addressing the evaporation rate, movement of the evaporation front, mole fraction, and concentration distributions of the chemicals involved in the VOC transport with the following sequence. First, the validity of the numerical model on predicting the evaporation front of a pure NAPL, i.e., toluene, residing in soil is assessed by comparing to the analytical solution. Second, the effect of initial mole fraction on the NAPL evaporation and the evolutions of the mole fraction distributions of benzene and toluene are studied. Third, the evaporation front for different chemicals, namely carbon tetrachloride and toluene, is examined. Finally, using the analytical solution for single VOC the effect of the effective diffusion coefficient, whose value depends on soil parameters and VOC chemical properties, on the moving speed of evaporation front is investigated. Soil parameters are listed in Table 1 and the chemical and physical characteristics of benzene, toluene, and carbon tetrachloride are given in Table 2. The depth of the lower bound $L$ is chosen as 5 m, the total number of nodes $N$ is 10,000, and the time interval $dt$ is 0.1 s in the finite difference approximation.

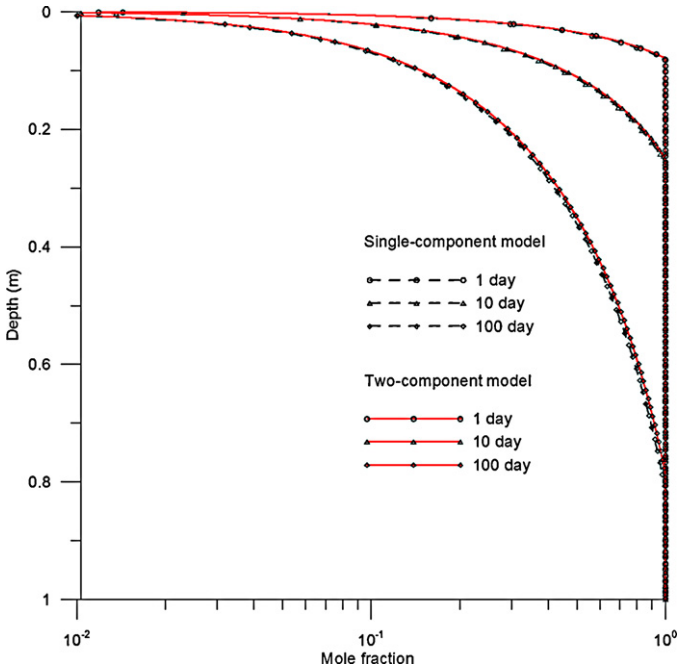


**Fig. 2.** Evolution of mole fraction of a VOC predicted by the analytical solution and numerical model at various evaporation times.

## 3. Results and discussion

### 3.1. Model verification

Fig. 2 shows the mole fraction distributions of toluene versus depth predicted by the analytical solution denoted as dashed lines and by the numerical model denoted as solid lines at various evaporation times. The symbols of circle, triangle, and rhombus represent the mole fractions at times 1, 10, and 100 days, respectively. The figure shows that the curves predicted by the analytical and numerical approaches are fairly close, revealing that the present numerical approach can adequately produce the result similar to that of the analytical solution. The moving speeds of the front $U_f$ estimated by Eq. (43) are $8.296 \times 10^{-2}$, $2.624 \times 10^{-2}$, and $8.296 \times 10^{-3}$ m/day at times 1, 10, and 100 days, respectively. It shows that the moving speed decreases rapidly at early time and then slowly as time increases.

### 3.2. Initial mole fraction for two-component NAPL

Fig. 3a–c shows the mole fraction distributions of benzene and toluene versus depth at 100 days as the initial mole fraction of benzene (component one, $u_1$) is 0.2, 0.5, and 0.8, respectively. The evaporation front of the NAPL reaches 0.860, 0.931, and 1.002 m below the surface with $u_1 = 0.123$, 0.310 and 0.498 at 100 days for $u^0 = 0.2, 0.5$, and 0.8, respectively. The figures show that the depth of the front increases with the initial mole fraction of benzene, revealing that the moving speed of the front depends on the initial mole fraction. Furthermore, the mole fraction of benzene increases with depth until reaching $u_1 = u^0$; on the other hand, the mole fraction of toluene increases with depth above the front but decreases below the front until reaching $u_2 = 1 - u^0$. The results show the evolution of mole fraction distributions of each component along the soil depth and demonstrate the use and ability of the present model. At the evaporation front, the toluene concentration has a negative gradient in both upward and downward directions, indicating that the depletion of toluene occurs due to diffusion in both directions (i.e., forward and backward diffusion). The backward diffusion of

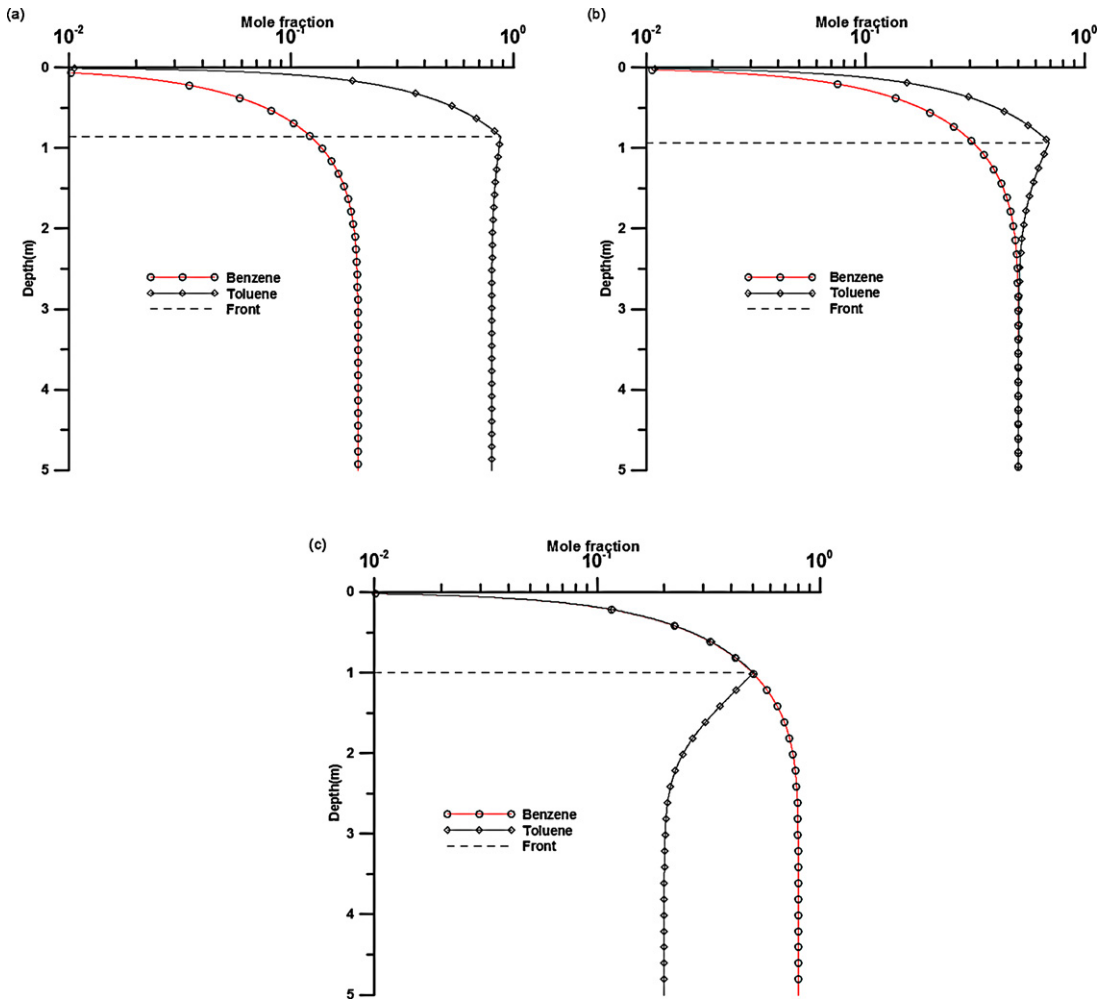


**Fig. 3.** Mole fraction distributions along soil depth at 100 days for two VOCs predicted by the numerical model as the initial mole fraction of benzene equals to (a) 0.2, (b) 0.5, and (c) 0.8.

toluene increases with the initial mole fraction of benzene causing higher difference between the mole fractions of toluene at the evaporation front and the initial toluene mole fraction value.

### 3.3. Different VOCs

Fig. 4 shows the distributions of normalized total concentration along the soil depth at 100 days predicted by the analytical solution for carbon tetrachloride and toluene, respectively. Note that the normalized total concentration is defined as $C_T(z,t)/C_T^0$. The solid lines with circle and triangle represent the concentration distribution of carbon tetrachloride and toluene, respectively. This figure indicates that the vaporization of toluene is significantly lower than that of carbon tetrachloride which reflects the facts that toluene has a lower molecular weight and liquid density and lower saturated vapor pressure and Henry's law constant than those of carbon tetrachloride as listed in Table 2. As a result, the depth of the evaporation front of toluene (0.813 m) is far less than the depth of carbon tetrachloride (1.659 m) at 100 days.

### 3.4. Effective diffusion coefficient

Fig. 5 shows the depth and moving speed of the evaporation front versus evaporation time for $D_E = 10^{-10}$, $10^{-9}$, $10^{-8}$, and $10^{-7}$ m$^2$/s. Notice that the vertical axis at the right-hand side in Fig. 5 presents logarithmic value of the moving speed of the front. It shows a significant difference among the depth and moving speed of the front with $D_E = 10^{-7}$ m$^2$/s and others. The effective diffusion coefficients for benzene, toluene and carbon tetrachloride are on the order of $10^{-7}$ to $10^{-8}$ m$^2$/s if based on the data presented in Tables 1 and 2. However, for soils with high moisture content or with low porosity, this coefficient value can be decreased to one or two orders of magnitude. Consequently, the moving speed of the

**Table 2**
Chemical properties of carbon tetrachloride, toluene, and benzene [35].

| Property | Symbol | Carbon tetrachloride value | Toluene value | Benzene value |
|---|---|---|---|---|
| Molecular weight (g/mole) | $M$ | 153.8 | 92.1 | 78.1 |
| NAPL density (g/m$^3$) | $\rho R$ | $1.584 \times 10^6$ | $8.62 \times 10^5$ | $8.79 \times 10^5$ |
| Saturated vapor pressure (kPa) | $P$ | 12.13 | 2.9 | 10.3 |
| Henry's law constant | $K_H$ | 0.958 | 0.26 | 0.22 |
| Organic carbon partition coefficient (m$^3$/g) | $K_{oc}$ | $1.1 \times 10^{-4}$ | $1.4 \times 10^{-4}$ | $8.3 \times 10^{-5}$ |

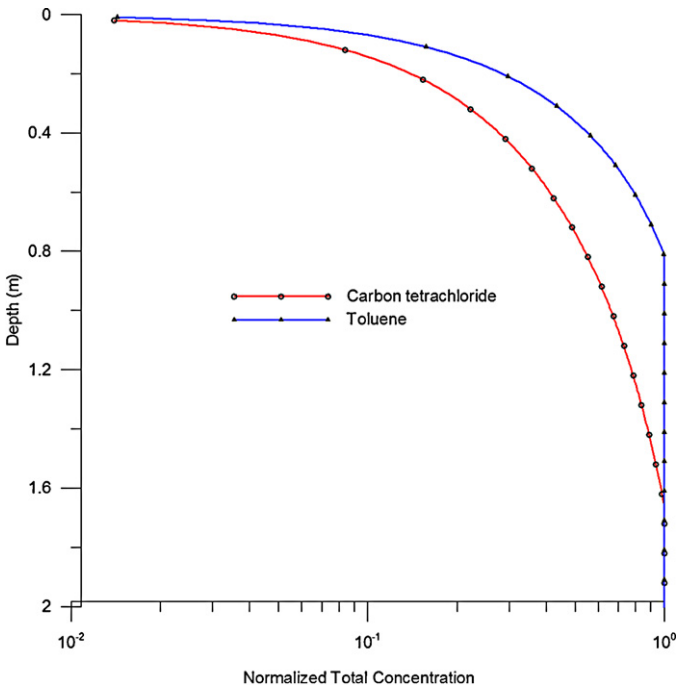


**Fig. 4.** Concentration distribution of a chemical along soil depth at 100 days assessed by the analytical solution.

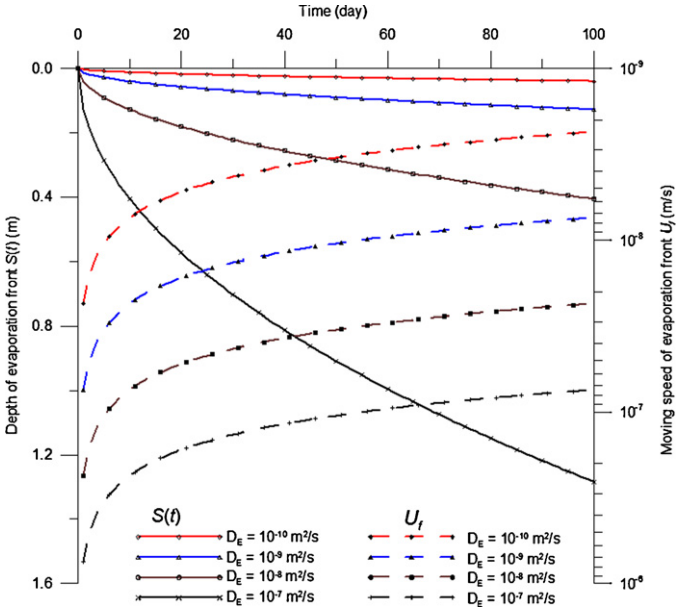


**Fig. 5.** Depth ($s(t)$) and moving speed ($U_f$) of evaporation front versus time for different effective diffusion coefficients assessed by the analytical solution.

evaporation front of the NAPL is greatly reduced as presented in Fig. 5.

## 4. Conclusions

This paper presents a two-component model to describe the mole fraction distributions of VOCs and the evaporation front of NAPL comprised of two VOCs in unsaturated soils. For simulating the mass spreading of VOCs in the region where the NAPL fully evaporates, zero-concentration is chosen as the upper boundary condition and a sharp moving boundary representing the evaporation front of NAPL is the lower boundary. In the region below the front where the NAPL exists, the upper boundary is the evaporation front while the lower boundary is relatively far away from the front and thus chosen at infinity. The model is then solved by the finite difference method with a moving grid approach for predicting the front location and concentration distributions of VOCs in these regions. The numerical model is also used to analyze the evaporation time of VOC and assess the influences of initial mole fraction, soil porosity as well as chemical volatility on VOC migration. In addition, the two-component model is further simplified to a single-component model and solved analytically by Boltzmann's transformation with a moving boundary. Analytical expressions are also developed for the front location and its moving speed as functions of evaporation time. The expression indicates that the depth of the evaporation front from the soil surface is proportional to the square root of volatilization time, while the contaminant gas phase concentration in the region above the evaporation front is governed by the error function.

These developed models are further used to assess the effects of initial mole fraction of two-component NAPL, different VOCs and effective diffusion coefficients on the concentration distributions of VOCs, the location as well as the moving speed of the evaporation front. The results reveal that downward back diffusion process of less volatile component is the governing factor dominating the evaporation front velocity. Back diffusion effect is more pronounced as the initial mass fraction of the more volatile component is higher or as the vapor pressure of the less volatile compound is higher.

## Acknowledgements

This study was partly supported by the Taiwan National Science Council under the grants NSC 99-2221-E-009-062-MY3, NSC 100-2221-E-009-106, and NSC 101-3113-E-007-008. The authors would like to thank two anonymous reviewers for their valuable and constructive comments that help improve the clarity of our presentation.

## References

[1] M. Christophersen, M.M. Broholm, H. Mosbaek, H.K. Karapanagioti, V.N. Burganos, P. Kjeldsen, Transport of hydrocarbons from an emplaced fuel source experiment in the vadose zone at Airbase Værløose, Denmark, J. Contam. Hydro. 81 (1-4) (2005) 1–33.
[2] M. Oostrom, C. Hofstee, R.J. Lenhard, T.W. Wietsma, Flow behavior, residual saturation formation of liquid carbon tetrachloride in unsaturated heterogeneous porous media, J. Contam. Hydro. 64 (1-2) (2003) 93–112.
[3] W.J. Ferguson, A. Kaddouri, A mass conservative non-isothermal subsurface three-phase flow model: formulation and application, Water Air Soil Poll. 153 (1-4) (2004) 269–291.
[4] G.A. Brusturean, T. Todinca, D. Perju, J. Carre, J. Bourgos, Soil clean up by venting: comparing between modelling and experimental voc removal results, Environ. Technol. 28 (10) (2007) 1153–1162.
[5] G.B. Davis, J.L. Rayner, M.G. Trefry, S.J. Fisher, B.M. Patterson, Measurement and modeling of temporal variations in hydrocarbon vapor behavior in a layered soil profile, Vadose Zone J. 4 (2) (2005) 225–239.
[6] C.A. Evans, K.S. McLeary, G.P. Patridge, R.S. Huebner, Modeling the impact of multicomponent VOCs on ground water using the Stefan–Maxwell equation, J. Am. Water Resour. As. 40 (2) (2004) 409–417.
[7] P.S. Lowell, B. Eklund, VOC. emission fluxes as a function of lateral distance from the source, Environ. Prog. 23 (1) (2004) 52–58.
[8] R.W. Falta, I. Javandel, K. Pruess, P.A. Witherspoon, Density-driven flow of gas in unsaturated zone due to evaporation of the volatile organic compounds, Water Resour. Res. 25 (10) (1989) 2159–2169.
[9] J. Massmann, D. Farrier, Effects of atmospheric pressure on gas-transport in the vadose zone, Water Resour. Res. 28 (3) (1992) 777–791.
[10] H.K. Karapanagioti, P. Gaganis, V.N. Burganos, P. Hohener, Reactive transport of volatile organic compound mixtures in the unsaturated zone: modeling and tuning with lysimeter data, Environ. Modell. Softw. 19 (5) (2004) 435–450.
[11] F.D. Tillman, J.W. Choi, J.A. Smith, A comparison of direct measurement and model simulation of total flux of volatile organic compounds from the subsurface to the atmosphere under natural field conditions, Water Resour. Res. 39 (10) (2003) 1284.

[12] S. Panday, P.S. Huyakorn, MODFLOW SURFACT. A state-of-the-art use of vadose zone flow and transport equations and numerical techniques for environmental evaluations, Vadose Zone J. 7 (2) (2008) 610–631.
[13] H.K. Yoon, A.J. Valocchi, C.J. Werth, Effect of soil moisture dynamics on dense nonaqueous phase liquid (DNAPL) spill zone architecture in heterogeneous porous media, J. Contam. Hydro. 90 (3–4) (2007) 159–183.
[14] Q. Liao, X. Tian, R. Chen, X. Zhu, Mathematical model for gas–liquid two-phase flow and biodegradation of a low concentration volatile organic compound (VOC) in a trickling biofilter, Int. J. Heat. Mass Trans. 51 (7–8) (2008) 1780–1792.
[15] M.O. Rivett, G.P. Wealthall, R.A. Dearden, T.A. McAlary, Review of unsaturated-zone transport and attenuation of volatile organic compound (VOC) plumes leached from shallow source zones, J. Contam. Hydro. 123 (3–4) (2011) 130–156.
[16] W.A. Jury, W.F. Spencer, W.J. Farmer, Behavior assessment model for trace organics in soil: I. Model description, J. Environ. Qual. 12 (4) (1983) 558–564.
[17] W.A. Jury, D. Russo, G. Streile, H.El Abd, Evaluation of volatilization by organic chemicals residing below the soil surface, Water Resour. Res. 26 (1) (1990) 13–20.
[18] J.S. Lin, L.M. Hildemann, A nonsteady-state analytical model to predict gaseous emissions of volatile organic compounds from landfills, J. Hazard. Mater. 40 (3) (1995) 271–295.
[19] C.A. Shoemaker, T.B. Culver, L.W. Lion, M.G. Peterson, Analytical models of the impact of two-phase sorption on subsurface transport of volatile chemicals, Water Resour. Res. 26 (4) (1990) 745–758.
[20] S.R. Yates, S.K. Papieri, F. Gao, J. Gan, Analytical solutions for the transport of volatile organic chemicals in unsaturated layered systems, Water Resour. Res. 36 (8) (2000) 1993–2000.
[21] Y. Sun, J.N. Petersen, T.A. Buscheck, J.J. Nitao, Analytical solutions for reactive transport of multiple volatile contaminants in the vadose zone, Transport Porous Med. 49 (2) (2002) 175–190.
[22] J. Crank, Free and Moving Boundary Problems, Oxford Univ. Press, New York, 1984.
[23] T.F. Cheng, Numerical analysis of nonlinear multiphase Stefan problem, Comput. Struct. 75 (2000) 225–233.
[24] E. Vazquez-Nava, C. Lawrence, Thermal dissolution of a spherical particle with a moving boundary, Heat Transfer Eng. 30 (5) (2009) 416–426.
[25] S.S. Sazhin, P.A. Krutitskii, I.G. Gusev, M.R. Heikal, Transient heating of an evaporating droplet, Int. J. Heat Mass Transfer. 53 (2010) 2826–2836.
[26] M.Y. Corapcioglu, A.L. Baehr, A compositional multiphase model for groundwater contamination by petroleum products: 1. Theoretical considerations, Water Resour. Res. 23 (1) (1987) 191–200.
[27] A.L. Baehr, M.Y. Corapcioglu, A compositional multiphase model for groundwater contamination by petroleum products: 2. Numerical solution, Water Resour. Res. 23 (1) (1987) 201–213.
[28] F.D. Tillman, J.A. Smith, Design and laboratory testing of a chamber device to measure total flux of volatile organic compounds from the unsaturated zone under natural conditions, J. Contam. Hydro. 75 (1–2) (2004) 71–90.
[29] R.J. Millongton, J.M. Quirk, Permeability of porous solids, Trans. Faraday Soc. 57 (1961) 1200–1207.
[30] P. Hohener, C. Duwig, G. Pasteris, K. Kaufmann, N. Dakhel, H. Harms, Biodegradation of petroleum hydrocarbon vapors: laboratory studies on rates and kinetics in unsaturated alluvial sand, J. Contam. Hydro. 66 (1-2) (2003) 93–115.
[31] J. Zaidel, A. Zazovsky, Theoretical study of multicomponent soil vapor extraction: propagation of evaporation-condensation fronts, J. Contam. Hydro. 37 (1999) 225–268.
[32] E. Javierre, F.J. Vuik, S. Vermolen, van der Zwaag, A comparison of numerical models for one-dimensional Stefan problems, J. Comput. Appl. Math. 192 (2006) 445–459.
[33] H.S. Carslaw, J.C. Jaeger, Conduction of Heat in Solids, 2nd ed., Clarendon, Oxford, 1959.
[34] H.D. Yeh, Theis' solution by nonlinear least-squares and finite-difference Newton's method, Ground Water 25 (6) (1987) 710–715.
[35] R.H. Perry, D.W. Green, J.Q. Maloney, Perry's Chemical Engineers' Handbook, 7th ed., McGraw-Hill, New York, 1997.